

Bioinspired multi-responsive soft actuators controlled by laser tailored graphene structures

Heng Deng, Cheng Zhang, Jheng-Wun Su, Yunchao Xie, Chi Zhang, and Jian Lin*

Department of Mechanical & Aerospace Engineering, University of Missouri-Columbia, Columbia, Missouri 65211, USA.
E-mail: LinJian@missouri.edu

1. Experimental Section

1.1 Fabrication of PVDF/LIG/PI actuators

Commercial PI film was scribed into LIG by DLW using a desktop CO₂ laser system. The pulse width of the laser was ~14 μs. The laser power was fixed at 14 W during the processing. The LIG patterns were first designed using AutoCAD, and then DXF files were loaded onto the software that controls the movement of the laser beam. To fabricate PVDF films 2 g of PVDF powder (Kynar Flex® 761) was dispersed in 8 g of *N,N*-dimethylformamide (DMF) in a 20-ml bottle and then heated at 80 °C by vigorous magnetic stirring until complete dissolution of the PVDF powder. The PVDF/DMF solution was then cooled to room temperature and ready for use. After that, the prepared PVDF/DMF solution was spin-coated at 800 rpm for 30 s on the surface of the LIG. The whole film was then kept in a vacuum box for 1 min to let the PVDF/DMF be penetrated into the pores of the LIG. After that, the PVDF/DMF soaked LIG/PI film was heated on a hotplate at 120 °C to evaporate the DMF solvent. Then, the LIG/PVDF film was peeled from the PI film and cut into the desired shapes. Finally, PI tapes were attached to LIG/PVDF film on the side of LIG. To fabricate electrothermal actuators, Cu electrodes were adhered to silver ink that was painted to the LIG electrodes to realize good electrical connection.

1.2 Fabrication of PVA/LIG/PI actuators:

The process for fabricating LIG is the same to previously stated one. Then 1 g of PVA powder was dispersed in 9 g of water in a 20-ml bottle and heated at 90 °C by vigorous magnetic stirring

until complete dissolution of the PVA powder. The PVA aqueous solution was then cooled to room temperature and ready for use. Then the prepared PVA aqueous solution was spin-coated at 400 rpm for 30 s on the surface of the LIG. The whole film was then kept in a vacuum box for 1 min to let the PVA aqueous solution be penetrated into the pores of the LIG. After that, the PVA soaked LIG/PI film was heated on a hotplate at 80 °C to evaporate the water. Then, the LIG/PVA film was peeled from the PI film and cut into the desired shapes. Finally, PI tapes were attached on the LIG surface.

1.3 Characterization

Morphology of the LIG was characterized by a Hitachi S-4800 SEM. Optical cross-section image of the PLP actuators and optical images of the PVDF/LIG films under thermal stimuli or acetone were taken using a microscope (MU130, AmScope). Graphical analysis was done using the software of AmScope. The thermal images were obtained by using a thermal camera (FLIR, T330). The videos and photographs of the responsive behaviors of the actuators were taken using a smart phone.

1.4 Calculation of energy efficiency

The energy efficiency of the PLP actuators can be defined as the generated elastic energy density divided by the electrical energy density. Given that the most part of the PVDF is penetrated into the LIG network, we consider the PVDF/LIG mixture as one single layer in the calculation. In this case, the tri-layer structure can be approximated as a bilayer structure of PI and PVDF/LIG mixture. Thus, the elastic energy density of the PLP actuator can be calculated by using the following equation:

$$W_1 = \frac{[E_3 t_3^2 (3t_2 + t_3) + E_2 t_2^2 (3t_3 + t_2)][E_2^2 t_2^4 + E_3^2 t_3^4 + 2E_2 E_3 t_2 t_3 (2t_2^2 + 2t_3^2 + 3t_2 t_3)]}{36E_2 E_3 t_2^2 t_3^2 (t_3 + t_2)} \left(\frac{1}{\rho}\right)^2$$

where W_1 is the elastic energy density, $1/\rho$ is the curvature (2.5 cm^{-1}), t_2 and t_3 are the thickness of PI layer ($25 \text{ }\mu\text{m}$) and LIG/PVDF mixture ($54 \text{ }\mu\text{m}$) respectively, E_2 and E_3 are the Young's modulus of PI

layer (2.425 GPa) and LIG/PVDF mixture (0.317 GPa) respectively. The Young's modulus of the PI layer and LIG/PVDF mixture are measured by a material testing machine at a stretching rate of 1.67 mm/s.

The calculated elastic energy density is $7.388 \times 10^4 \text{ J/m}^3$. Assuming the actuation time of 5 s, the total electrical energy density applied to the actuator is given by:

$$W_2 = p \cdot \tau$$

where W_2 is the electrical energy density, p is the power density (68.02 mW/mm^3), τ is the actuation time (5 s). The calculated electrical energy density is $3.4 \times 10^8 \text{ J/m}^3$.

Hence, the energy efficiency η is given by:

$$\eta = W_1 / W_2$$

The energy efficiency of η is then calculated to be 0.0217%.

2. Supplemental Figures

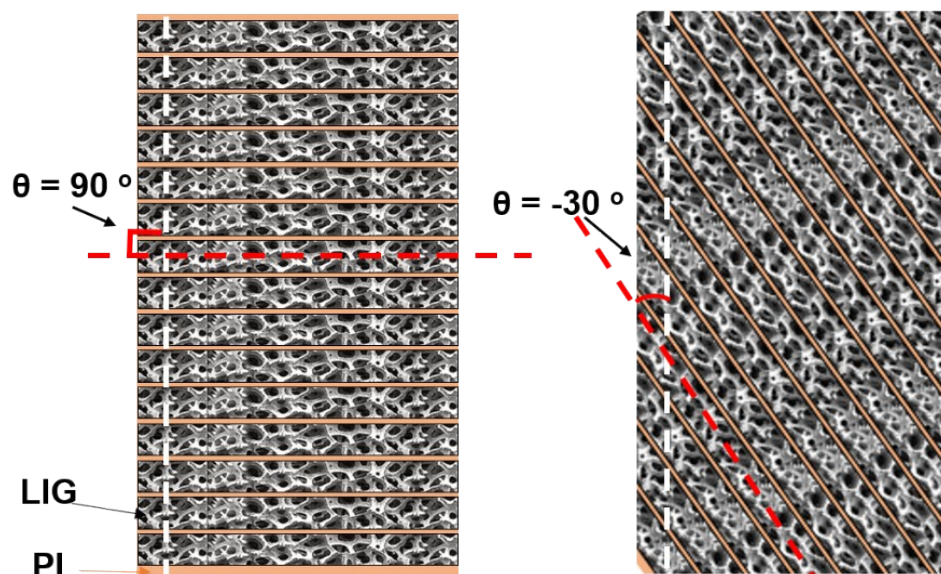


Figure S1. Schematic of alignment angle (θ) which is defined by the LIG orientation (red dot line) and the longitudinal direction (white dot line) of the resulting film.

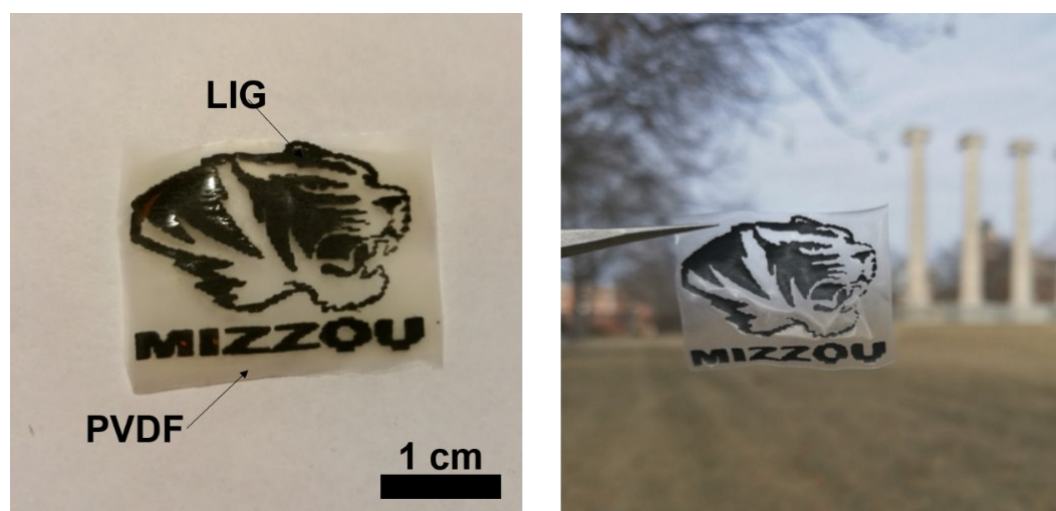


Figure S2. Photographs of the LIG/PVDF bimorph which was peeled off from a PI film. The black pattern (tiger) was LIG, and the transparent substrate was PVDF. The LIG patterns remain intact after being transferred from PI to PVDF.

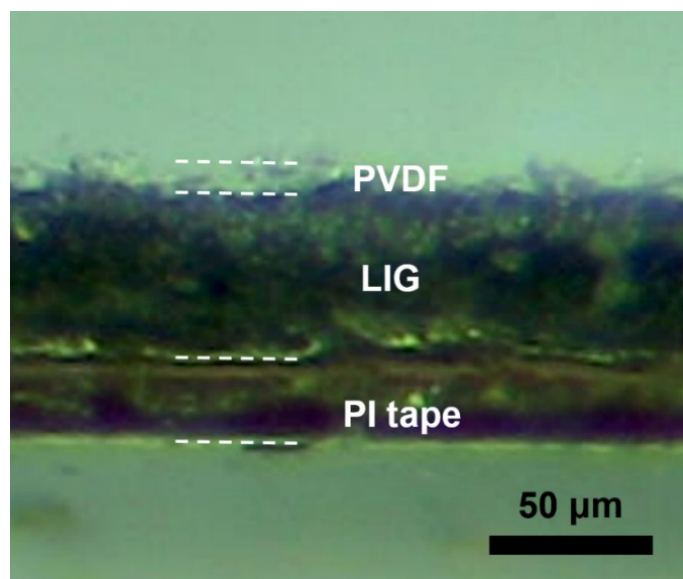


Figure S3. Cross-section image of the LIG/PVDF/PI film, in which these layers were compactly contacted with each other.

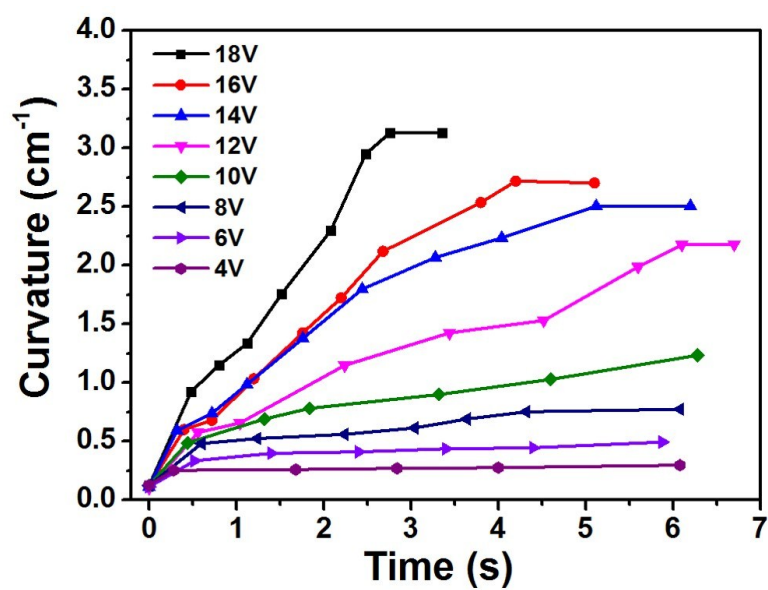


Figure S4. Plot of curvatures versus time for the PLP actuators stimulated by different electrical voltages.

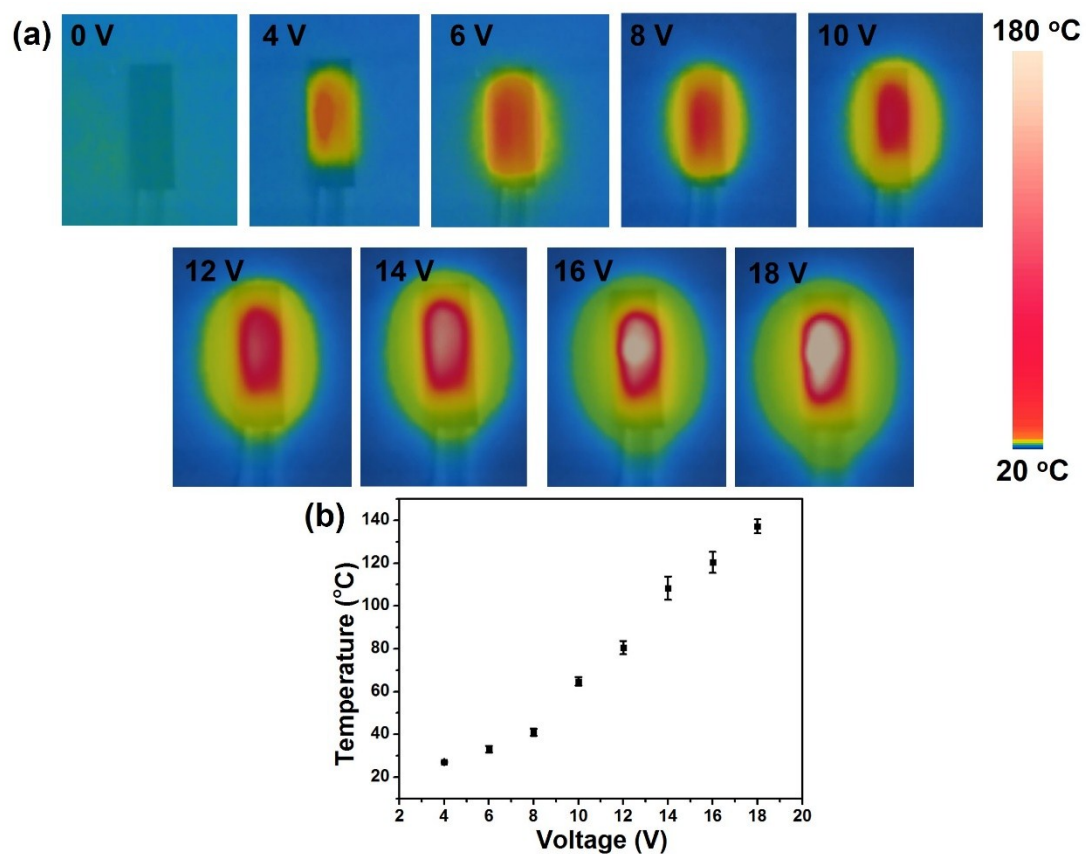


Figure S5 (a) Thermal images of a PLP actuator stimulated by different electrical voltages from 0 V to 18 V. The actuator was fixed on glass slide to facilitate the observation. (b) Plot of average temperature of the PLP actuator versus electrical voltages. The temperature was measured from the above thermal images.

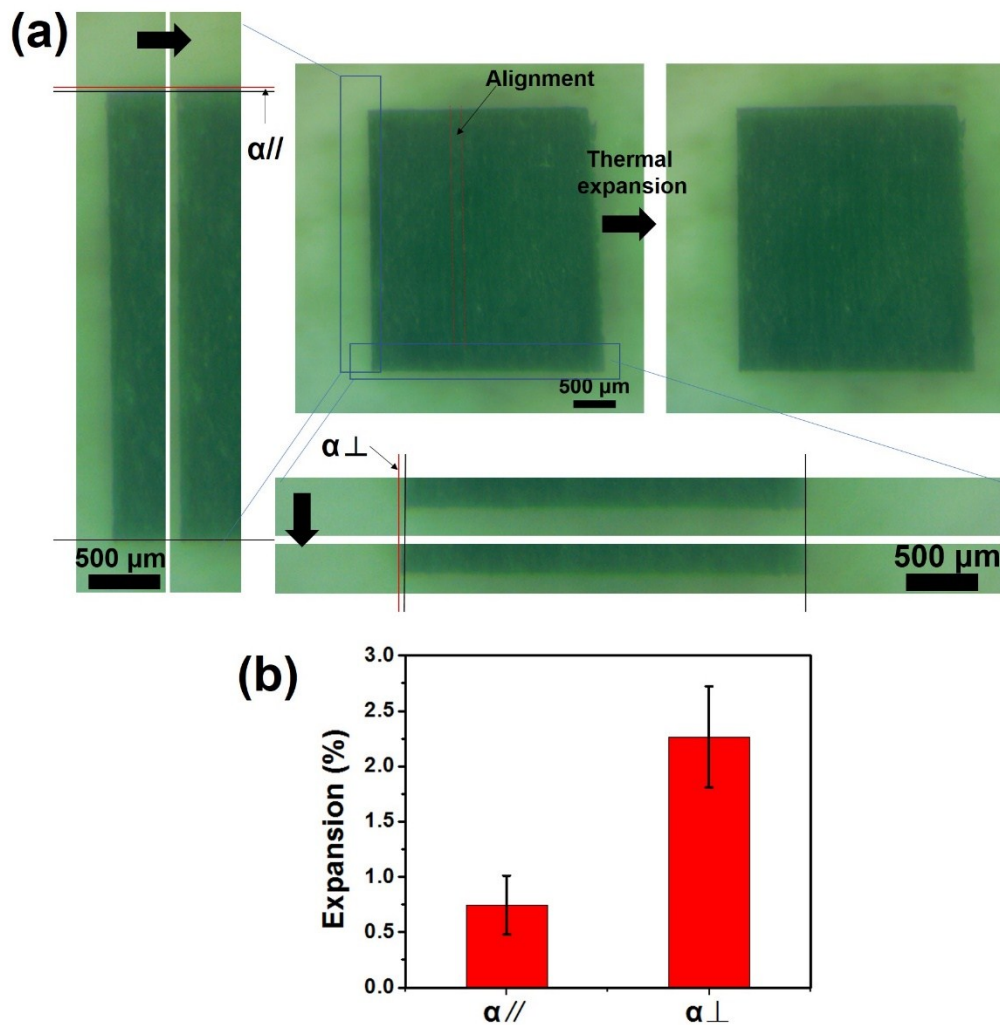


Figure S6. (a) Photographs of a PVDF/LIG bimorph under 120 °C. As shown in these images, the transverse expansion strain (α_{\perp}) is larger than longitudinal expansion strain ($\alpha_{//}$). The expansion strain is expressed as the ratio of changed length ΔL to the original length L of the investigated sample. (b) Statistical results of the transverse expansion strain (α_{\perp}) and longitudinal expansion strain ($\alpha_{//}$) under 120 °C stimulus.

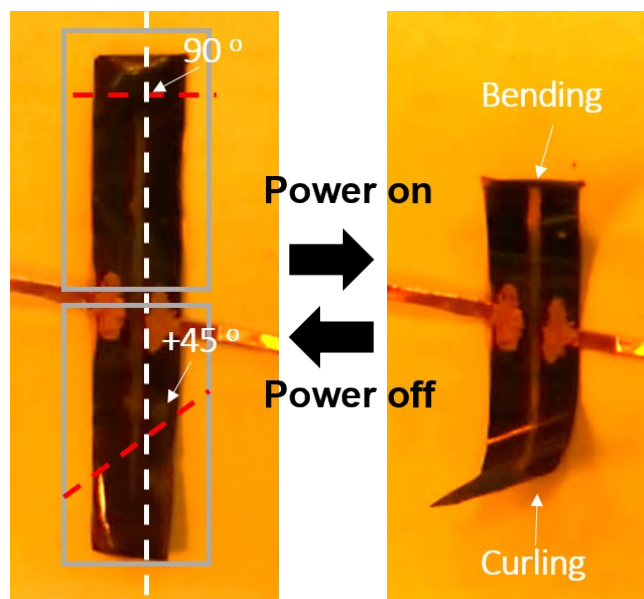


Figure S7. Photographs of a PLP actuator integrated with two different LIG circuit patterns ($\theta = 90^\circ$ and $+45^\circ$). Upon electrical stimulation, the local bending and helical curling motions were simultaneously achieved.

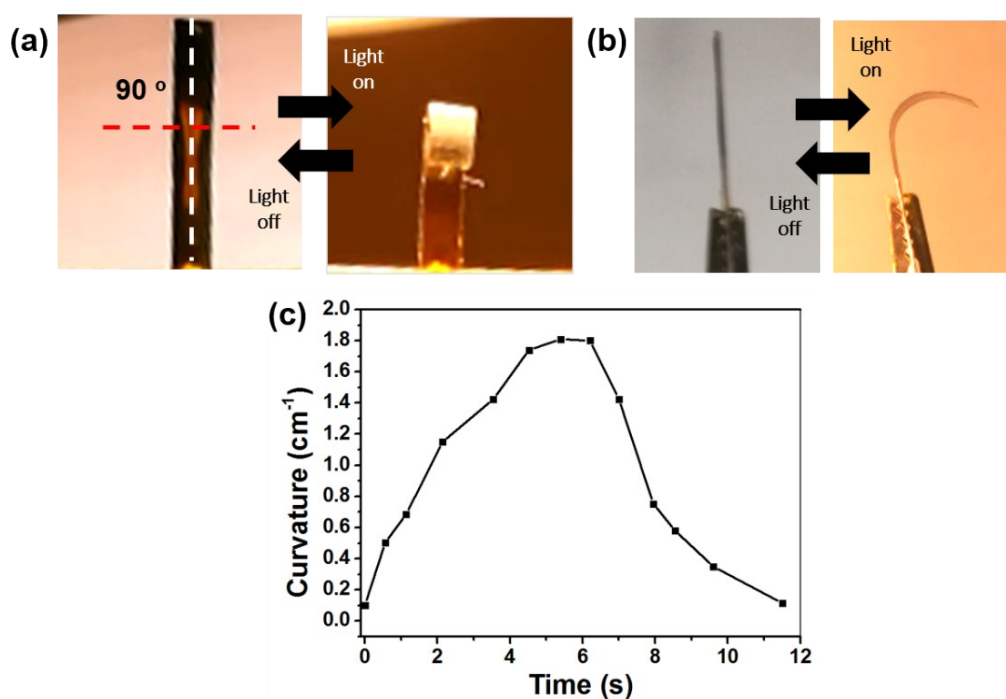


Figure S8. (a) Top-view (a) and side-view (b) Photographs of a responsive PLP actuator ($\theta = 90^\circ$) under light irradiation (The lamp is 4 cm distance from the actuator). (c) Plot of bending curvatures versus time for a PLP actuator under light irradiation (The lamp is 4 cm distance from the actuator.).

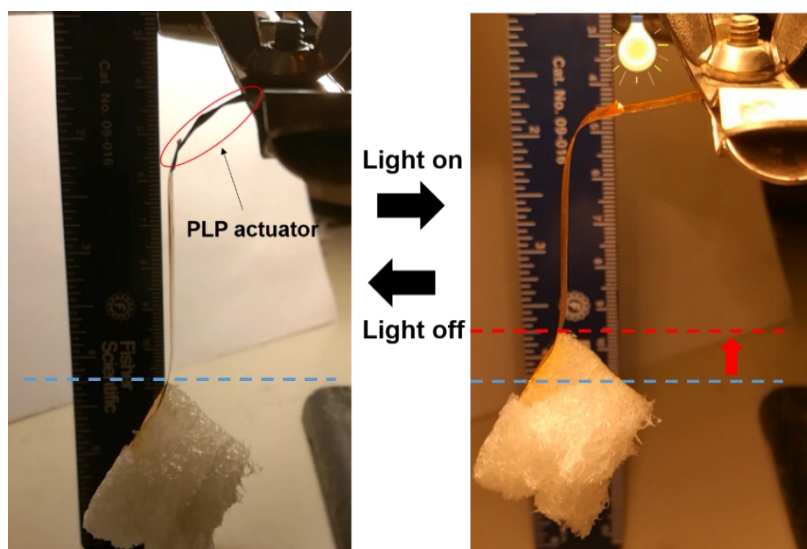


Figure S9. Photographs of a PLP actuator ($\theta = 90^\circ$) in lifting a plastic foam upon stimulation of light irradiation (The lamp is 4 cm distance from the actuator.). The blue dot line represents the original position of the plastic foam. The red dot line represents the final position of the plastic foam.

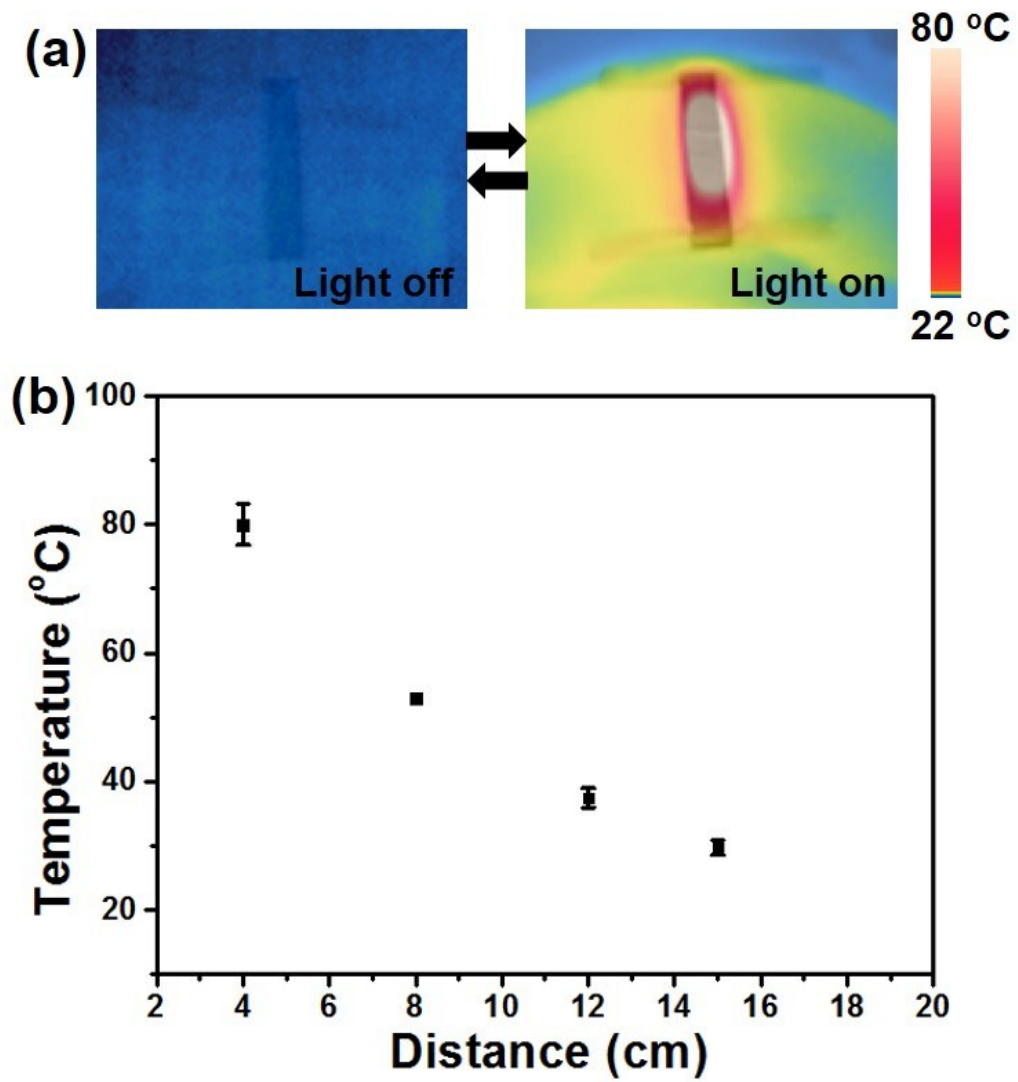


Figure S10. (a) Thermal image of a PLP actuator stimulated by a lamp which is 4 cm distance from the actuator. The actuator was fixed on glass slide to facilitate the observation. (b) Plot of average temperature of a PLP actuator versus the distance between the lamp and the actuator.

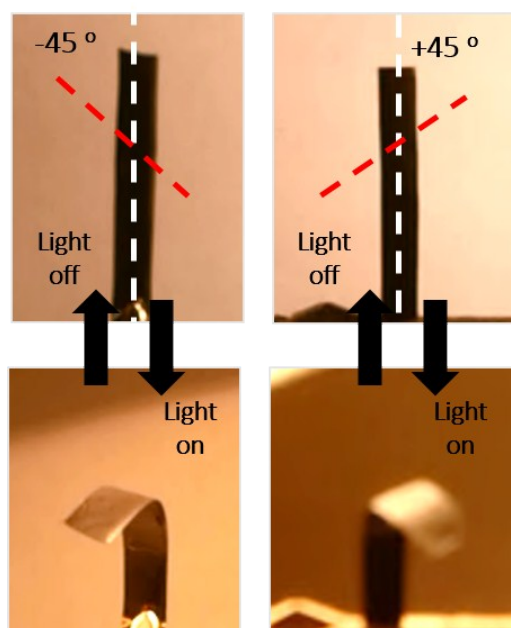


Figure S11. A top-view photographs showing a responsive process of a PLP actuator ($\theta = -45^\circ$ and $+45^\circ$) under light irradiation (The lamp is 4 cm distance from the actuator.).

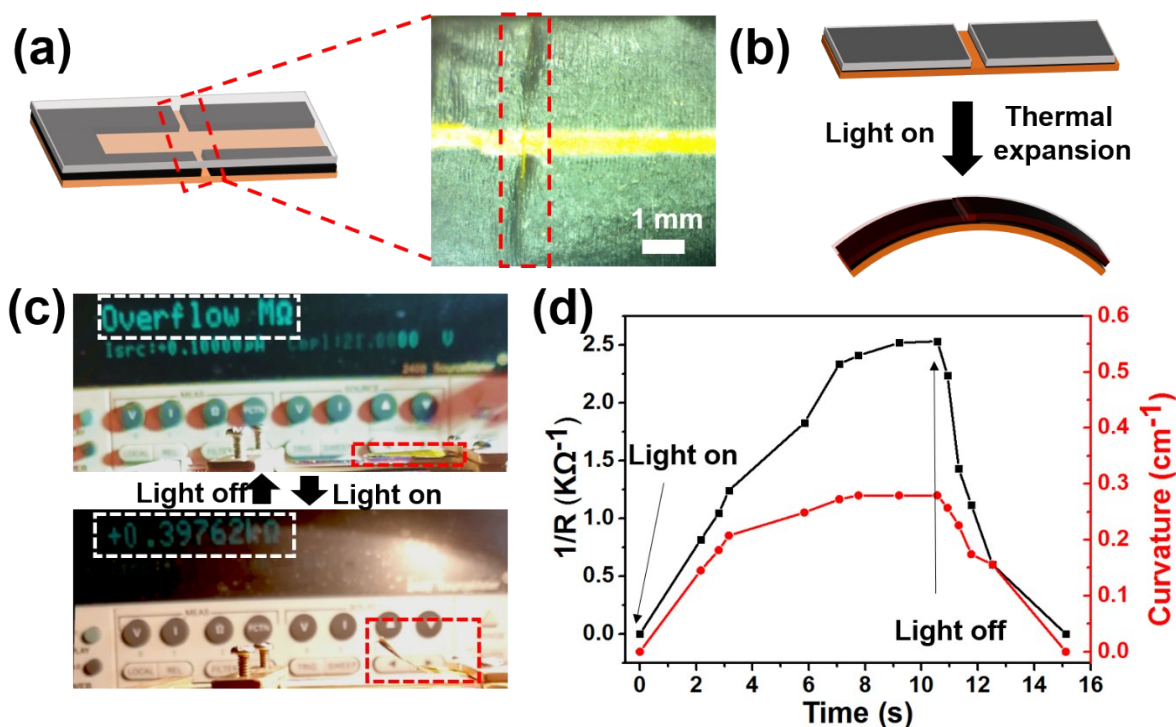


Figure S12. (a) A scheme and optical images of a crease made on a PLP actuator. (b) A scheme showing that bad connection between LIG is reconnected under thermal expansion. (c) Optical images showing the bending motion of a PLP actuator (red dotted box) and its change of resistance (white dotted box) when responding to light. (d) Plot of reciprocal value of resistance (black line) and bending curvatures (red line) versus time for a PLP actuator under light irradiation (The lamp is 10 cm distance from the actuator).

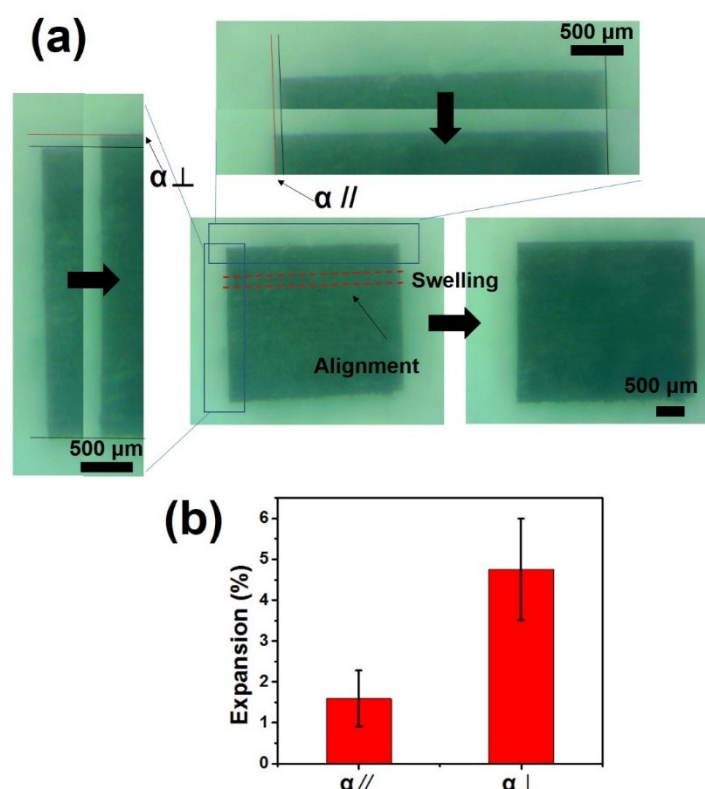


Figure S13. (a) Photographs of a PVDF/LIG bimorph in acetone. As shown in these images, after swelling, the transverse expansion strain (α_{\perp}) is larger than longitudinal expansion strain (α_{\parallel}). (b) Statistical results of the transverse expansion strain (α_{\perp}) and longitudinal expansion strain (α_{\parallel}) after swelled in acetone.

Table S1. Performance comparison of PLP actuators with recently reported multi-responsive soft actuators.

	This work (PVDF/LIG/PD)	AgNWsPEDOT:PSS/ Paper (Reference 28)	BOPP/graphite/paper (Reference 37)
Electrothermal actuation	Voltage: 14 V Response time: 5 s Curvature: 2.5 cm ⁻¹	Voltage: 8 V Response time: 20 s Curvature: 1.1 cm ⁻¹	Voltage: 30V Response time: 10 s Curvature: 2.6 cm ⁻¹
Photothermal actuation	Light source: 150 W lamp (distance 4 cm) Response time: 5s Curvature: 1.8 cm ⁻¹	Light source: 100 W lamp (distance 30 cm) Response time: 30 s Displacement: 19 mm	Light source: NIR light (300 mW/cm ²) Response time: 10 s Curvature: 1.9 cm ⁻¹
Actuation responsive to chemical stimuli	Acetone vapor (30 kPa, 25 °C)	Moisture (RH of 60 %)	Moisture (RH of 70%)